

ESA AO/1-6367/10/NL/AF

“GOCE+ Theme 3: Air density and wind retrieval using GOCE  
data”

# Data Set User Manual

For data set version 2.0

Prepared by: Eelco Doornbos – TU Delft / KNMI

April 8, 2019



# Change log

- July 18, 2013 First issue, coinciding with data release v1.2.
- September 23, 2013 Second issue, coinciding with data release v1.3. Section 1.3 has been updated to describe the changes in the data processing introduced with v1.3 data.
- June 5, 2014 Third issue, coinciding with data release v1.4. Section 1.3 has been updated to describe the changes in the data processing introduced with v1.4 data.
- July 5, 2016 Fourth issue, coinciding with data release v1.5. Section 1.3 has been updated to describe the changes in the data processing introduced with v1.5 data.
- April 5, 2019 Fifth issue, coinciding with data release v2.0. Section 1.3 has been updated to describe the changes in the data processing introduced with v2.0 data.



# Contents

<b>1</b>	<b>Data products</b>	<b>9</b>
1.1	Density and wind data time series . . . . .	9
1.1.1	File name and file format . . . . .	9
1.1.2	Structure . . . . .	9
1.2	Plots of gridded data . . . . .	11
1.3	Versions . . . . .	11
1.3.1	Version history . . . . .	14
1.4	Density scale considerations . . . . .	16
<b>2</b>	<b>Data usage</b>	<b>19</b>
2.1	Measurement environment . . . . .	19
2.1.1	Orbit geometry . . . . .	19
2.1.2	Solar and geomagnetic activity . . . . .	21
2.1.3	Eclipses . . . . .	21
2.2	Considerations for accuracy and data usage . . . . .	21
2.2.1	Thruster activation data . . . . .	21
2.2.2	Density accuracy and scale uncertainty . . . . .	22
2.2.3	Effect of thrust level variations at low thrust on density accuracy . . . . .	23
2.2.4	Interpretation of the crosswind vector . . . . .	23
2.2.5	Crosswind accuracy . . . . .	24
2.2.6	Error estimates . . . . .	24
2.3	Vertical wind data . . . . .	24
2.4	Deorbit phase data . . . . .	24



# Introduction

This manual is intended for users interested in the thermosphere density and wind data derived from the GOCE mission. The manual will explain the contents of the data set, will supply some additional information which might be of interest to users, and it will provide some warnings on limitations of the data. For detailed information on the data processing and validation, readers are referred to the Final Report, Algorithm Theoretical Basis Document and Validation Report of the GOCE+ Theme 3 study, which will be made available for download, as one PDF file, together with the data set and this manual. Many of the improvements in the current version 2.0 of the dataset are also documented in recent publications [March et al., 2018, 2019, Visser et al., 2018, 2019a,b].

## Acknowledgements

The GOCE data processing for thermosphere density and wind was performed as part of an ESA Support To Science Element (STSE) funded study (contract 4000102847/N-L/EL), with support from ESA's GOCE team (special thanks to Alberto Bigazzi and Rune Floberghagen). The ESA study manager for this study was Michael Kern. Work on version 2.0 of the data set was done under the ESA GOCE High-Level Processing Facility contract. The study partners who worked on these project are:

- Eelco Doornbos, Tim Visser, Gunther March, Pieter Visser, Jose van den IJssel and Joao Encarnacao at Delft University of Technology (TU Delft), Astrodynamics and Space Missions research group, at the Faculty of Aerospace Engineering, located in Delft, The Netherlands;
- Sean Bruinsma at Centre National d'Études Spatiales (CNES), in Toulouse, France;
- Bent Fritsche and Georg Koppenwallner at Hypersonic Technology Goettingen (HTG), Katlenburg-Lindau, Germany.

Sadly, Georg Koppenwallner passed away in October 2012. At the time of writing Eelco Doornbos has started working at KNMI (the Royal Netherlands Meteorological Institute) and can be reached at [eelco.doornbos@knmi.nl](mailto:eelco.doornbos@knmi.nl).

## Questions

For questions on how to access the data, users can contact the ESA Earth Observation helpdesk at [eohelp@esa.int](mailto:eohelp@esa.int). The homepage of ESA Earthnet Online can be found at <http://earth.esa.int>.

Questions related to scientific use of the data and the contents of this user manual can be addressed to Eelco Doornbos at KNMI, via [eelco.doornbos@knmi.nl](mailto:eelco.doornbos@knmi.nl).

# Chapter 1

# Data products

The main data product is in the form of time series of density and wind speeds. These will be shown in Section 1.1. Section 1.2 shows the gridded data, which can be used for quick identification of data availability, data quality and special events, such as geomagnetic storms. More detailed information for users of the data is provided in Chapter 2.

## 1.1 Density and wind data time series

### 1.1.1 File name and file format

The density and wind data time series are supplied as plain text files, with each file storing one month worth of data. Because the data are stored as plain text, they should be readable on any operating system, and can be imported for further processing using many different software packages.

On the download server, the files are compressed and stored in an archive, so they have to be unpacked before use.

An example of the full name of an uncompressed text files is:

```
goce_denswind_ac082_v2.0_2009-11.txt
```

This filename contains the following information: the satellite name (goce), the data product name (denswind), the value of the energy accommodation coefficient used in the processing (ac082, meaning that  $\alpha_E = 0.82$ ), the data major and minor version number (v2.0) and the year and month numbers for the data in this file (2009-11 for November 2009).

### 1.1.2 Structure

The plain text data files contain a short header at the top of the file, followed by many data records, in subsequent lines. A data record is defined as a single line in the text file, which provides data for a single epoch. Each record is subdivided into various fields, which are separated by spaces. Each field contains a numerical or text value for a certain variable. A sample of the start of one data file is supplied in Figure 1.1.

```

# GOCE density and wind data for accommodation coefficient 0.82, exported on: 2019-02-28 09:44:34 UTC at TU Delft
# Data processing funded by ESA STSE under contract 4000102847/NL/EL GOCE+ Theme 3: "Air density and wind retrieval using GOCE data"
# Version 2.0 Funded by: ESA's GOCE High Level Processing Facility (HLPF) contract
# Contact: ESA Earth Observation helpdesk, eohelp@esa.int, http://earth.esa.int/
# Column 1:      Date (yyyy-mm-dd)
# Column 2:      Time (hh:mm:ss.sss)
# Column 3:      Time system
# Column 4:      f10.3 Altitude (m)
# Column 5:      f8.3 Geodetic longitude (deg)
# Column 6:      f7.3 Geodetic latitude (deg)
# Column 7:      f6.3 Local solar time (h)
# Column 8:      f7.3 Argument of latitude (deg)
# Column 9:      e12.6 Density (kg/m3)
# Column 10:     f8.2 Eastward component of crosswind speed (m/s)
# Column 11:     f8.2 Northward component of crosswind speed (m/s)
# Column 12:     f8.2 Upward component of crosswind speed (m/s)
# Column 13:     e12.6 Absolute RSS density error (kg/m3)
# Column 14:     f8.2 Absolute RSS wind error (m/s)
# Column 15:     f2.0 Flag: 0 = Data ok, 1 = Data possibly affected by outliers, missing data, or filter initialization
# Column 16:     f2.0 Flag: 0 = Data ok, 1 = Data possibly affected by eclipse transition
# Column 17:     f2.0 Flag: 0 = Ascending (dusk) pass, 1 = Descending (dawn) pass
# Column 18:     f2.0 Flag: 0 = ion thruster assumed active, 1 = ion thruster assumed inactive
# Format string: (a27,1x,f10.3,1x,f8.3,1x,f7.3,1x,f6.3,1x,f7.3,1x,e12.6,1x,f8.2,1x,f8.2,1x,f8.2,1x,e12.6,1x,f8.2,1x,f2.0,1x,f2.0,1x,f2.0)
# Date/time      alt      lon      lat      lst      arglat  dens_x_it  cr_wnd_e  cr_wnd_n  cr_wnd_u  denserror  winderro  no  ec  as  th
#               m        deg      deg      h        deg      kg/m3      m/s       m/s       m/s       kg/m3      m/s
2010-04-01 00:00:00.000 UTC 281826.559 290.862 -66.290 19.391 67.046 1.396595e-11 85.66 28.40 0.98 8.440641e-13 16.69 0 1 0 0
2010-04-01 00:00:10.000 UTC 281688.952 290.359 -65.652 19.360 293.621 1.388836e-11 91.44 29.69 3.69 8.389991e-13 16.82 0 1 0 0
2010-04-01 00:00:20.000 UTC 281547.274 289.879 -65.013 19.331 294.288 1.392647e-11 94.52 30.05 3.94 8.409784e-13 16.80 0 1 0 0
2010-04-01 00:00:30.000 UTC 281401.609 289.419 -64.373 19.303 294.956 1.408613e-11 93.75 29.19 6.20 8.504885e-13 16.63 0 1 0 0
2010-04-01 00:00:40.000 UTC 281252.038 288.978 -63.732 19.276 295.623 1.418576e-11 96.13 29.36 6.61 8.561692e-13 16.54 0 1 0 0
2010-04-01 00:00:50.000 UTC 281098.648 288.554 -63.089 19.251 296.291 1.441751e-11 100.80 30.23 6.12 8.696256e-13 16.33 0 1 0 0
2010-04-01 00:01:00.000 UTC 280941.525 288.147 -62.446 19.226 296.958 1.468922e-11 105.06 30.97 5.16 8.855958e-13 16.09 0 0 0 0
2010-04-01 00:01:10.000 UTC 280780.758 287.756 -61.801 19.203 297.626 1.487075e-11 108.31 31.40 7.42 8.960520e-13 15.94 0 0 0 0
2010-04-01 00:01:20.000 UTC 280616.436 287.379 -61.156 19.181 298.293 1.489861e-11 114.10 32.56 6.34 8.972626e-13 15.97 0 0 0 0
2010-04-01 00:01:30.000 UTC 280448.652 287.015 -60.509 19.159 298.960 1.518635e-11 116.37 32.67 -0.38 9.141885e-13 15.71 0 0 0 0
2010-04-01 00:01:40.000 UTC 280277.499 286.664 -59.862 19.139 299.628 1.525697e-11 117.14 32.39 4.93 9.187028e-13 15.67 0 0 0 0
2010-04-01 00:01:50.000 UTC 280103.072 286.324 -59.214 19.119 300.295 1.587811e-11 113.02 30.77 9.56 9.552712e-13 15.09 0 0 0 0

```

Figure 1.1 Example of the first lines of a time series data file, including the header and the first couple of data records.

## Header

The header lines are marked with a hash-sign (#) as the first character in the line. The first header lines contain attribution information and contact details. Subsequent header lines give a FORTRAN format specifier and description of each of the data fields (columns) in the data records that are to follow. The last three header lines contain the complete FORTRAN format specifier that was used for the output of the data, abbreviated column headings, and units for the data fields.

## Data records

The data records always start with a time tag, including the time system. The version 1.0 to 1.5 data files used time tags in GPS time, while the version 2.0 data is now provided with UTC time tags.

In subsequent columns, the data files contain information on the satellite orbit position, in the form of altitude, longitude, and geodetic latitude. These quantities are computed from the GOCE Precise Science Orbits (PSO), making use of the GRS-80 reference ellipsoid. The local solar time is currently computed from the longitude and time of day, and therefore represents an approximation to the mean local solar time only.

The argument of latitude is the angle along the orbit starting at the ascending node. It is also computed from the Precise Science Orbits, which are first converted to a True of Date inertial reference frame, and then converted to Keplerian orbit elements. The argument of latitude is computed as the sum of the argument of perigee and the true anomaly. It is a convenient angle for making the distinction between between ascending (270° to 360° and 0° to 90°) and descending arcs (90° to 270°), or to plot data which crosses

the poles (at around  $90^\circ$  for the North Pole and around  $270^\circ$  for the South Pole). This is done for the plots in the gridded data files, that are discussed in the next Section.

The last four columns in the data file contain the actual observations of density and crosswind.

## 1.2 Plots of gridded data

A secondary data product is the gridded data. The time-series data is binned as a function of epoch time on the X-axis and argument of latitude on the Y-axis. These grids are then made into monthly plots, provided in a single multi-page PDF document for the entire data set.

The gridded data are very useful for several purposes:

- Quick identification of data availability and data gaps. Data gaps are plotted in gray in all panels, while data that is available but that has been marked invalid is plotted in black in the top-right panel.
- Quick identification of data quality. Noisy data, outliers, jumps and biases are apparent as offsets in colour in the grids.
- Quick identification of geophysical signals in the data. Since the argument of latitude is closely related to the true geodetic latitude, patterns of changes in time at various latitudes become readily apparent in the plots.

Figure 1.2 shows an example of gridded density and wind data for the month of April 2010. From top to bottom the left-hand column shows the density data, the Eastward and upward crosswind components and time series of the  $ap$  geomagnetic activity index and  $F_{10.7}$  solar EUV radiation proxies. The addition of the activity index and proxy makes it easy to identify, for example, the geomagnetic storm on April 5, as the source of the density enhancement on that day. The right-hand column contains an overview of the data availability and flagging, the northward component of the crosswind, as well as a graph of the variation of the altitude of the satellite over the month.

The highest wind speeds can be found over the poles. The daily pattern at the poles is a result of the offset between the geomagnetic pole, to which the variations in the wind field are connected, and the geographic pole, to which the orbit geometry is tied.

Figure 1.3 shows all the processed data over the entire mission.

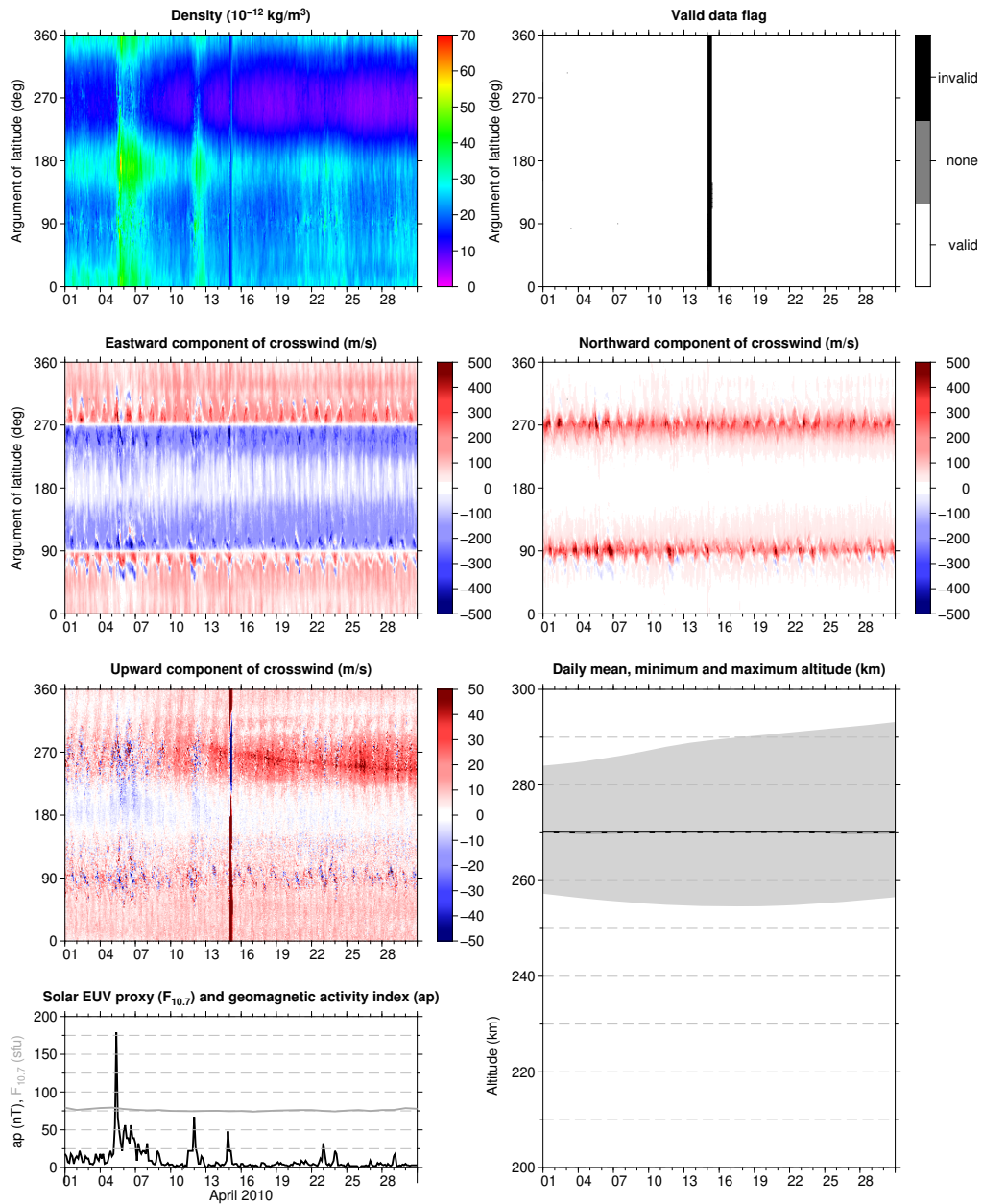
## 1.3 Versions

The data version is an indicator of the state of the software and models used in the data processing. The current version is v2.0. Versions, v1.0 and v1.1, were used for internal testing and validation, and were not released for distribution. Version v1.2 was the first public release.

Each new version number reflects updated processing software, implementing either more accurate algorithms and models, or bug fixes. It is important to always use a consistent data set, with a single version, and not mix older and newer data. Users are therefore recommended to check the version number of previously downloaded data, when downloading new data, and discard the older data if necessary.

Thermosphere density and crosswind speed  
along the GOCE orbit

April 2010



Version 2.0 – Data processing by Tim Visser, Eelco Doornbos, Gunther March and Pieter Visser at TU Delft  
Funded by ESA STSE GOCE+ Theme 3: "Air density and wind retrieval using GOCE data" and GOCE High-Level Processing Facility  
Contact for questions on technical and scientific issues: Eelco Doornbos, eelco.doornbos@knmi.nl  
Contact for questions on data access: ESA Earth Observation helpdesk, eohelp@esa.int, <http://earth.esa.int>

Figure 1.2 Example of one page of the gridded density and wind data file, for the month of April, 2010

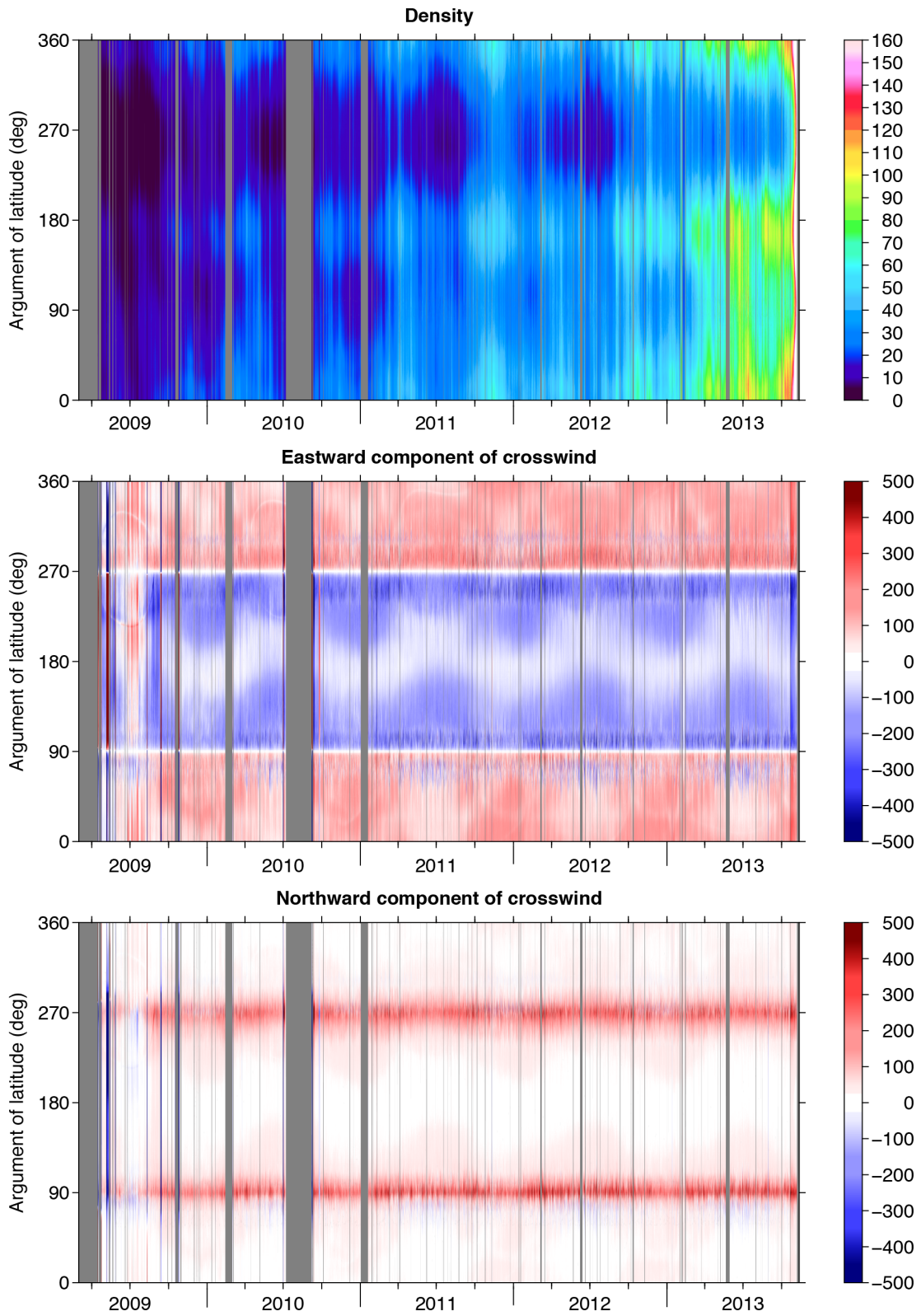


Figure 1.3 Gridded data for the entire mission.

### 1.3.1 Version history

The list below provides a short description of each of the data set versions, and the changes made with each new version.

**Version 1.0** First internal test version for initial validation, September 2012;

**Version 1.1** Second internal test version, February 2013. Extended dataset with more months; Improved accelerometer calibration; Adjusted thruster pointing; Data editing applied: removal of incorrect data after inspection of time series.

**Version 1.2** First release version, July 2013. Improved accelerometer calibration, leading only to negligible differences in density and wind with respect to Version 1.1. Improved data editing.

**Version 1.3** Second release version, September 2013. There were three changes:

1. Data editing of version 1.2 was only applied to the figures of gridded data. It was not applied to the time series data files. This has been corrected, resulting in removal of incorrect data for several periods, ranging from hours to days.
2. A bug in the iterative density and crosswind determination algorithm was fixed, leading to slightly different density and wind values. The bug was related to the projection of the HWM wind on the spacecraft body-fixed Z-axis (SBF-Z), described in equation (6.55) in the Algorithm Theoretical Basis Document (ATBD). This projected wind was added to the a-priori value, but was not subtracted when determining the final crosswind value in equation (6.52). Since the HWM model only supplies horizontal wind velocities, and the SBF-Z axis is kept closely aligned with the vertical direction, the wind component was of the order of a few tenths of 1 m/s.
3. The unit vector  $\hat{e}_{up}$  in equation (6.42) of the ATBD is now pointing in the vertical direction, defined by a reference ellipsoidal representation of the Earth. In earlier versions, this unit vector was aligned with SBF-Z. The small angle between SBF-Z and vertical is the result of pitch and roll motion of the satellite.

The combined effect of changes 2 and 3 on the data is dependent on the satellite's small pitch and roll angles, which continuously change over time. The mean effect is close to zero, while the standard deviations are of the order of 0.01% for the relative change in density and of the order of 2 m/s for the change in crosswind velocity.

**Version 1.4** Third release version, July 2014. This release includes data from the start to the end of GOCE's nominal mission operations, so from November 2009 until October 19, 2013. There have been numerous additional modifications to the data processing.

1. New input data: ESA made available new thruster data. This includes data from during the commissioning phase, before November 2009, data after May 2012 up to the end of the mission, and several additional passes of data which appeared as gaps in the earlier versions of the data set. Note that not all data has proved to be consistent with our models and data processing procedures.

For this reason, data from selected periods has been processed into density and wind data, but the results were in some cases excluded from this release. Most notably, this concerns the commissioning phase data (April to October 2009) and deorbit phase data (end of October and early November 2013). There is a possibility that this data will be added in a future release, when the inconsistencies have been studied and corrected.

2. New acceleration bias calibration functions. New bias calibration piecewise polynomial functions were created to fit through the daily bias value estimates. Because of this, the acceleration bias values for pre-existing data has also shifted slightly.
3. Error estimates have been added, based on an error propagation approach. The error estimates are the root-sum-square of various error contributions, computed from artificially introduced acceleration errors due to various known sources. More details are available in the Algorithms Theoretical Basis Document.
4. Four binary flag fields have been added. One flag indicates whether the satellite was on an ascending or descending pass. The other three flags can be used for quality control, because they represent the status of the ion thruster assembly used for drag free control, as well as whether there is a possibility of an eclipse transition.
5. Information on the optical properties of the GOCE solar arrays was received and implemented in the solar radiation pressure model. In addition, low drag data from during the commissioning phase allowed the determination of a solar radiation pressure model scale factor, and Y-axis acceleration correction. This has resulted in a reduction in the discrepancy between sunlit and shadow period crosswind data in 2010. Crosswind data in shadow has been affected the most.

**Version 1.5** Fourth release version, July 2016. In previous versions, the telemetry data field used to reconstruct the ion thruster acceleration was the `current.thrustfield` from the `AUX_NOM` data, which represents the output thrust as reported by the thruster electronics. For version 1.5, this has been changed to the field with the title `thrust_demand`, which represents the input to the thrusters. While the control loop for the ion thruster used a high data rate (10 Hz) for the input, the telemetry downlink is at a low data rate (0.125 Hz). Therefore, in the presence of noisy variations, the low rate downlinked input to the thruster actually provides a more accurate representation of the actual acceleration at the low rate used for computing the density and wind data than the reported thruster output.

**Version 2.0** The data has been reprocessed with a completely new implementation of the algorithms, as described by Visser et al. [2019a]. The algorithm makes use of a new satellite geometry and aerodynamic model representation, described by March et al. [2018], with a new setting of the aerodynamic energy accommodation coefficient  $\alpha_E = 0.82$  that was found through analysis described in March et al. [2019]. These new models result in an improved consistency of the wind data, as well as differences in density of a few percent with respect to the Version 1.5 data. Data processed with the old accommodation coefficient of 0.93, which might be useful

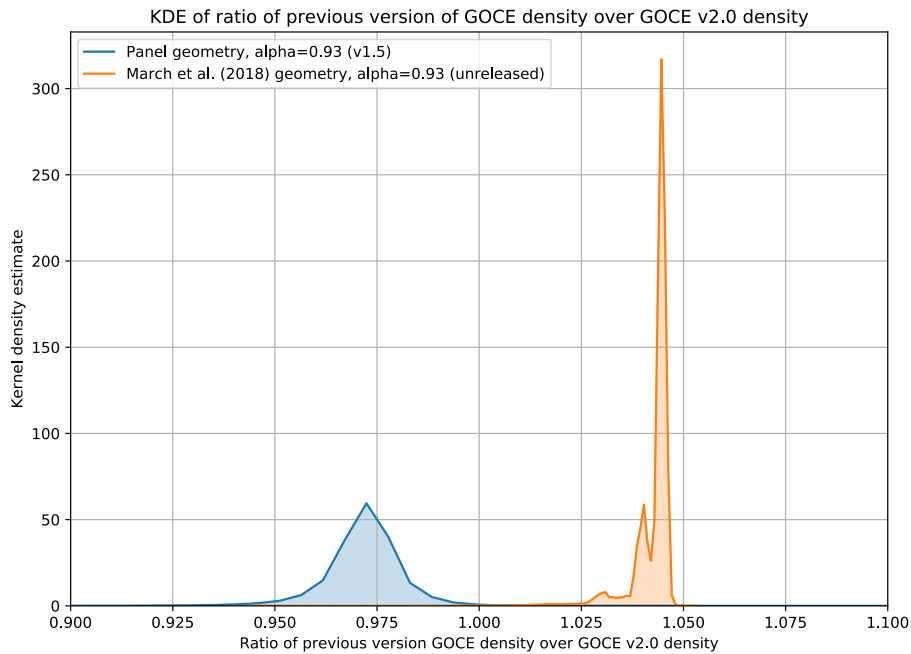


Figure 1.4 Kernel density estimates of the ratio of previous/alternative versions of GOCE densities over the current GOCE v2.0 densities.

for studies of satellite aerodynamics, are available from Eelco Doornbos, on request. The version 2.0 data also for the first time includes two versions of the dataset for the GOCE deorbit phase, from October 22 to November 10, 2013. Due to issues with the science data during this phase, one version, identified by the acronym DFACS (drag-free & attitude control system) is based on GOCE accelerometer data from the DFACS housekeeping channel. The second version (GPS only), is based on accelerations that were estimated in a Kalman-filter orbit determination approach using the mission’s GPS receiver data. This second version is less accurate and has a lower temporal resolution, but GPS data remained available until 7 hours before the satellite’s re-entry, while the accelerometer instruments were saturated and shut down many hours earlier. Users are advised that the new data contains new flags, that now have to be applied by the user, to filter out data of suspicious quality. The layout of the gridded data files have changed as well.

## 1.4 Density scale considerations

The changes made in version 2.0, to the representation of the satellite geometry and energy accommodation coefficient of the data, have an impact on the overall scale of the data.

Figure 1.4 shows how the old v1.5 data relates to the new data, in the form of a Kernel Density Estimate plot, which shows the distribution of the ratio of the two versions of the same measurements. Also included in the plot is a version of the data that includes the new high-fidelity geometry model from March et al. [2018], but with the old energy

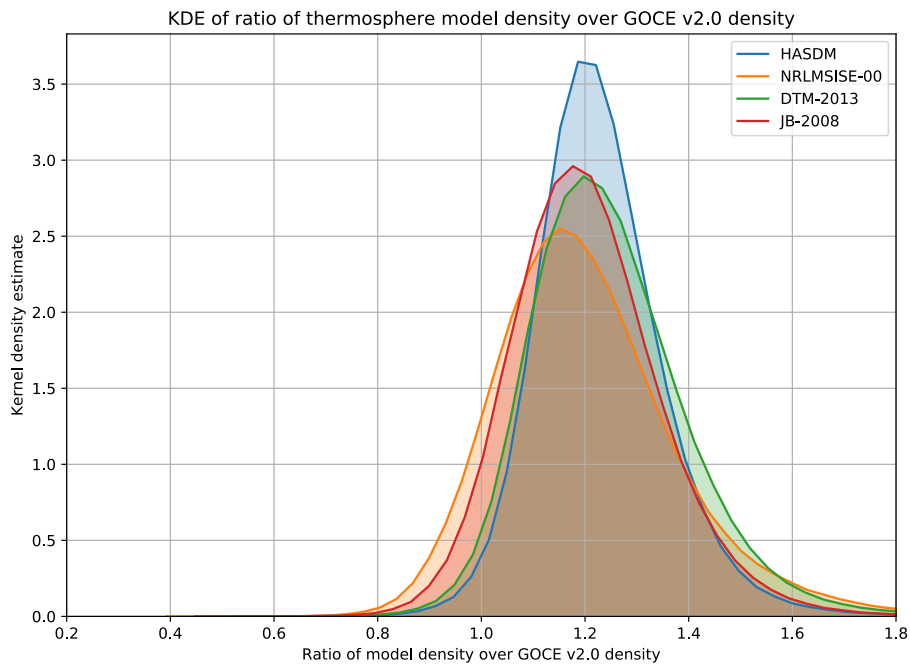


Figure 1.5 Kernel density estimates of the ratio of various empirical density models over the current GOCE v2.0 densities. Note the different axis scales, compared to Figure 1.4.

accommodation coefficient of 0.93 used in the computation.

The Figure shows that densities in the current version 2.0 dataset are on average approximately 3% larger than in the previous version 1.5. This is due to the densities becoming about 7% larger with the introduction of the high-fidelity geometry model, and subsequently about 4% smaller with the adjustment of the aerodynamic energy accommodation coefficient from 0.93 to 0.82. The spread around these offsets is only a few percent, and is mainly caused by the dependency of the changes in the geometry and aerodynamic model on the satellite attitude.

Figure 1.5 shows the distribution of the ratio of the density from various empirical models, over the v2.0 GOCE data, while Figure 1.6 compares the three versions of the data with just the HASDM model output.

The HASDM [Storz et al., 2005] output is based on assimilation of drag data from orbiting objects tracked by the US Space Surveillance Network contemporaneously with the GOCE mission. The JB-2008 model [Bowman et al., 2008] was used with solar indices version 5.4g, that were retroactively recalibrated. The DTM-2013 model [Bruinsma, Sean, 2015] is partly based on a previous version of the GOCE data, while the NRLMSISE-00 model [Picone et al., 2002] is completely independent.

On average, the models overestimate the density measured by GOCE by about 15-20%. This offset is based on the assumption that the GOCE measurements have been processed correctly. However, there is still a remaining uncertainty in the satellite aerodynamic modelling, that can likely only be fully resolved with dedicated in-space experiments in the future. Other major possible contributing factors to this discrepancy could

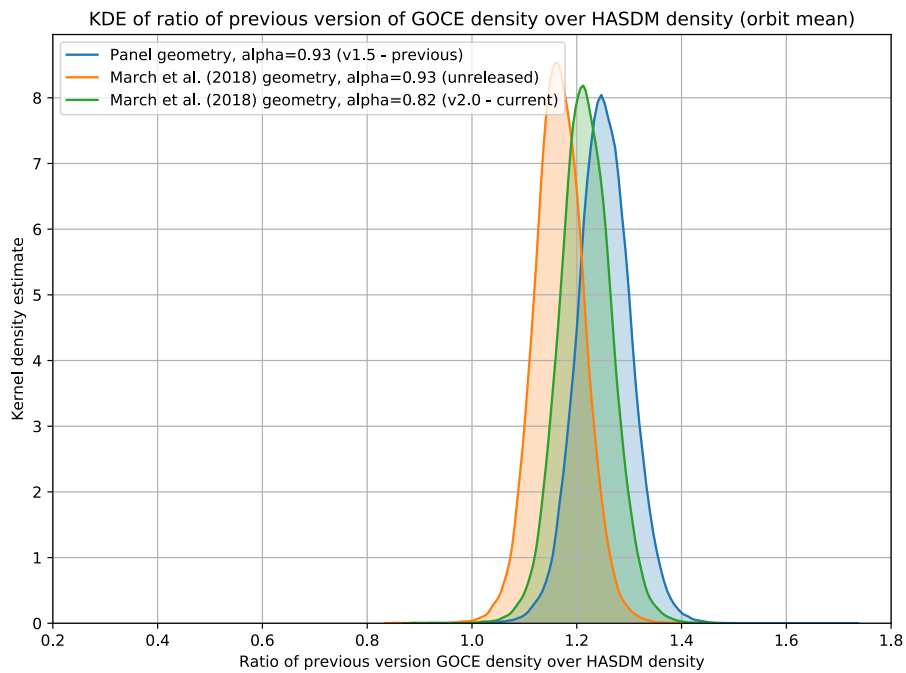


Figure 1.6 Kernel density estimates of the ratio of HASDM model output over the various GOCE density data set versions that were already shown in Figure 1.4.

be that the models do not incorporate long-term cooling of the thermosphere, and could be based on past drag data, processed using simplified geometry models and satellite aerodynamics assumptions.

## Chapter 2

# Data usage

This Chapter will provide practical background information and more in-depth information, which might be of interest for users of the GOCE density and crosswind data. Section 2.1 will give details on the orbit, solar activity and geomagnetic activity which together largely determine the environmental conditions in which the measurements were made.

### 2.1 Measurement environment

The measurement environment, both in terms of the orbit geometry and solar and geomagnetic activity conditions, during the course of the GOCE mission, will be discussed in the following paragraphs.

#### 2.1.1 Orbit geometry

The potential impact of the GOCE data on investigations and modelling work is largely determined by the GOCE orbit geometry and environmental conditions at the time of the measurements. Figure 2.1 shows the evolution of the GOCE orbital altitudes and local solar time at the nodes (equator crossings). The same information is included in the graphs for the CHAMP and GRACE satellites, for reference. The altitude is given as daily mean values (solid lines) of the altitude above the GRS-80 ellipsoid. In addition, the shaded areas indicate daily minimum and maximum altitude values. The mean altitude curves of course vary under the influence of drag and orbital control thruster activity (CHAMP and GOCE only). The variations in minimum and maximum altitude with respect to the mean are due to the flattening of the reference ellipsoid representing the oblate Earth, the eccentricity of the orbit, and the perigee rotation rate, caused by orbit perturbations.

The variation of the local solar time at the equator is due to orbital precession and the Earth's rotation around the Sun. The CHAMP and GRACE satellites both have a much stronger rate of the orbit plane with respect to the Sun than GOCE, which is near

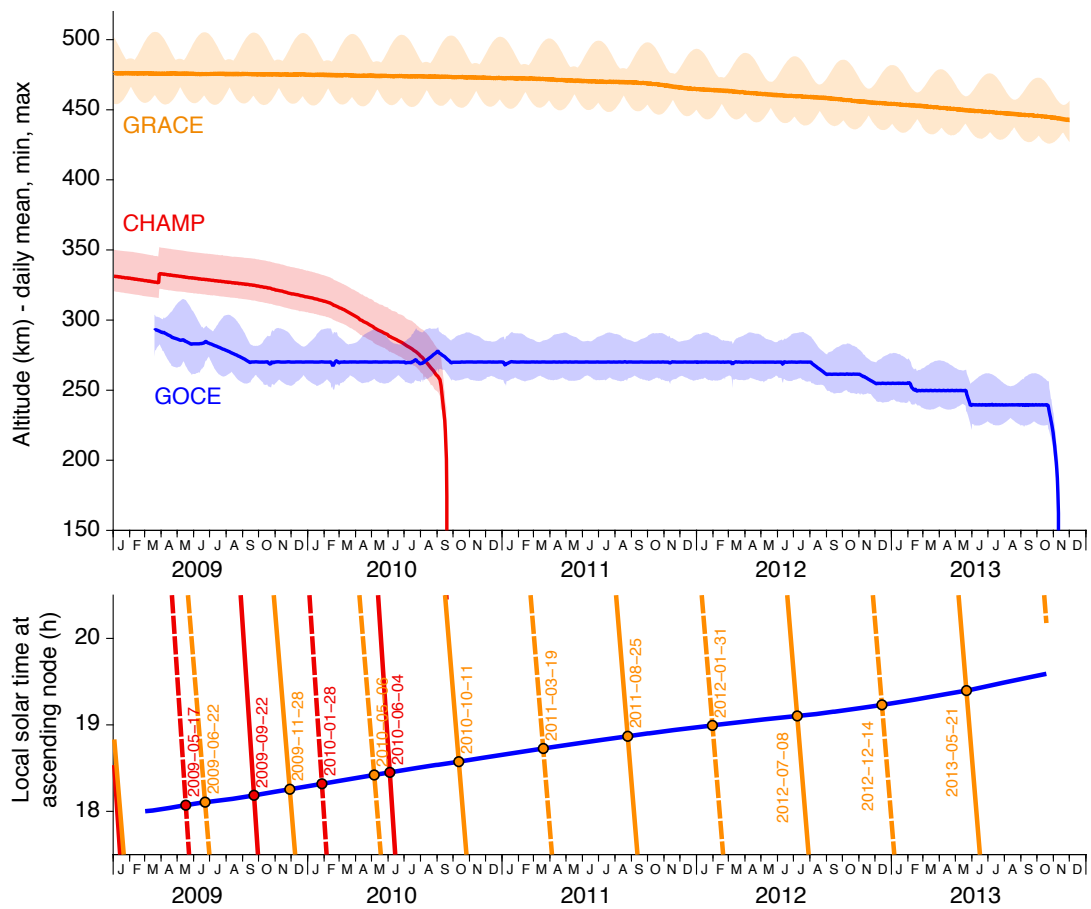


Figure 2.1 Orbital altitude and local solar time at equator crossings for GOCE, compared with CHAMP and GRACE.

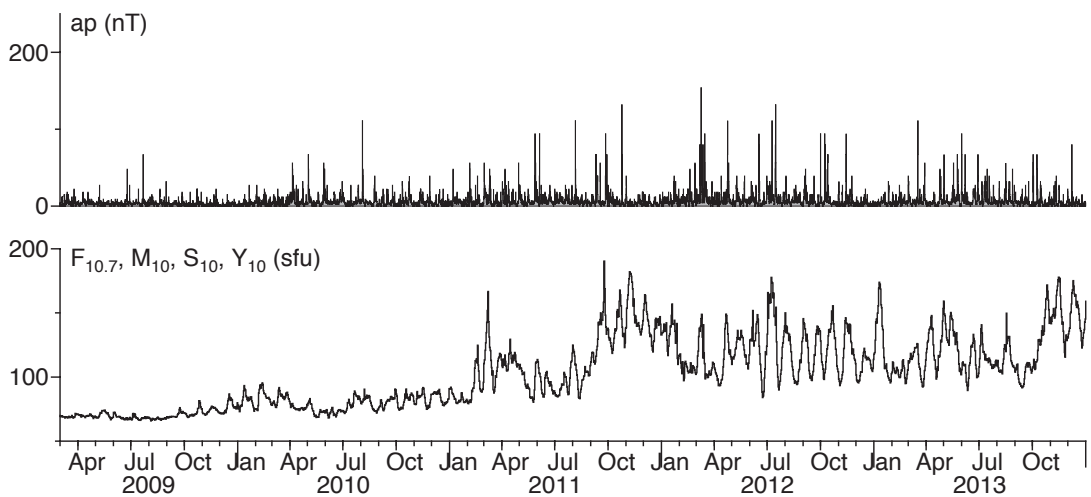


Figure 2.2 Time series of the ap geomagnetic activity index and the  $F_{10.7}$  solar EUV flux proxy.

sun-synchronous. The Figure indicates the dates at which the orbit of GOCE was nearly coplanar with one of the other two missions.

The GOCE altitude has been kept fixed at a very low level, which is not accessible for long durations without a drag free control system. The only major exceptions to the fixed altitude are the lowering manoeuvres at the start and end of the mission life, and during and after several on-board anomalies, where the drag free control system was commanded to keep the satellite as safe as possible during recovery operations.

The satellite was launched into a sun-synchronous dawn-dusk orbit, crossing the equator at 18:00 and 06:00 local solar time. Since launch, these equator crossing times have drifted during the course of the mission, due to orbit perturbations. The fixed low altitude and near sun-synchronous orbit are unique aspects of the mission, and need to be taken into consideration by users of the data.

### **2.1.2 Solar and geomagnetic activity**

Figure 2.2 shows an overview of how solar and geomagnetic activity evolved over the course of the mission. The mission started at the end of a period of extremely low solar activity. The intensity of solar EUV radiation has steadily increased during the current solar maximum, although the levels are still relatively low compared to earlier solar cycles. The clear 27-day variation in solar activity has become apparent during the solar maximum period.

There have been several geomagnetic storms during the GOCE mission lifetime until now.

### **2.1.3 Eclipses**

Figure 2.3 shows a graphical representation of the occurrence of solar eclipses by the Earth and Moon, during the course of the GOCE mission. Due to the fact that the orbit is not quite sun-synchronous, the eclipse periods have gotten longer during the course of the mission. The eclipses affect the radiation pressure accelerations. For the density determination, these are not important, as the magnitude of the radiation pressure accelerations are much smaller than the aerodynamic accelerations. For the crosswind determination this is a different matter, as the radiation pressure acceleration acts predominantly in the cross-track direction for GOCE. During full eclipses, the radiation pressure acceleration is absent, and so are radiation pressure model errors. But the exact modelling of eclipse transitions is difficult, due to the effect of the oblate Earth and refraction and absorption of Sunlight. Radiation pressure modelling errors can be large around these eclipse transitions, and the users of GOCE crosswind data should keep this in mind.

## **2.2 Considerations for accuracy and data usage**

### **2.2.1 Thruster activation data**

The density data from GOCE is comparable to existing data sets from the CHAMP and GRACE missions. The data processing algorithm is based on Doornbos et al. [2010]. The main difference with CHAMP and GRACE is the operation of the ion thruster, as part of the drag free control system, which is designed to keep the accelerations along the spacecraft's X-axis (it's length direction) at zero. In the algorithm of Doornbos et al.

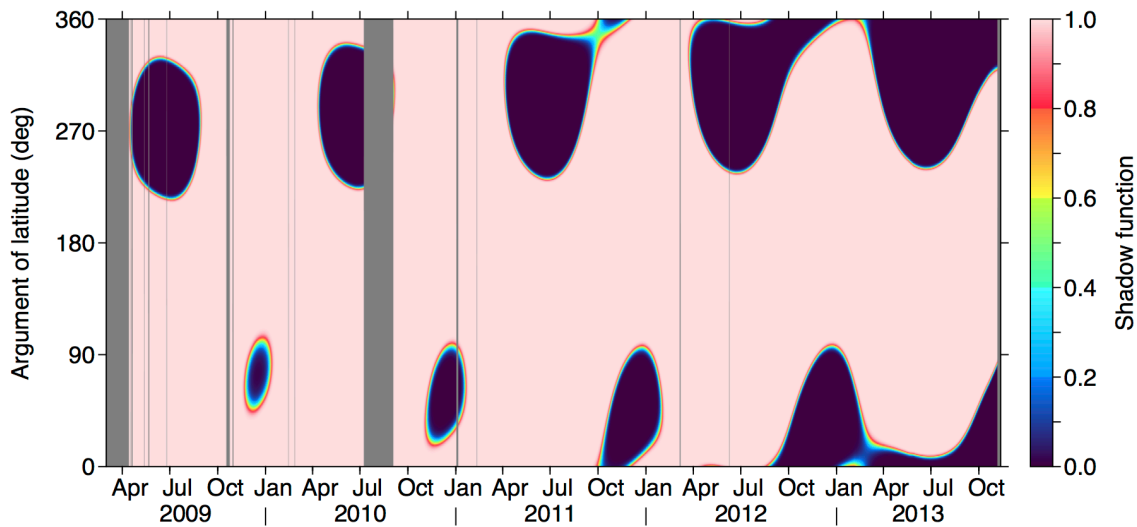


Figure 2.3 Time vs argument of latitude gridded plot of the so-called shadow function, which indicates whether the satellite is in full sunlight (1.0) or darkness behind the Earth (0.0). Note that due to the dusk-dawn orbit of GOCE, there are relatively long periods where the satellite is in semi-shadow. There are also a couple of occasions where the sunlight is partially or completely blocked by the Moon instead of the Earth.

[2010], this acceleration is subtracted from the accelerometer data, just like the radiation pressure acceleration, to arrive at the aerodynamic acceleration. Since the accelerometer X-axis data is almost always near zero, the information on the density for GOCE stems from the thruster activation data.

This thruster activation data is not part of the routine GOCE scientific data stream. Instead, it is part of the housekeeping data, originally intended only for checks on the health of the satellite and performance of its subsystems. The temporal resolution is therefore lower than that of the accelerometer data: the thruster activation is sampled for downlink only every 8 seconds, approximately, while the on-board algorithm that controls the thruster activation does so at a much higher rate. Due to this downlink sampling issue, some temporal details are lost. In the density and wind processing, the 8 second data is linearly interpolated to integer 10-second time steps, before further processing is applied. Of course, this sampling rate also limits the temporal resolution of the density data, and thereby the spatial resolution of the along-track density time series, which is approximately 80 km.

### 2.2.2 Density accuracy and scale uncertainty

According to Doornbos et al. [2010], errors in the geometry model and aerodynamic model of the satellite are the most important error sources in accelerometer-derived density data. Scale inconsistencies or errors in the density data of up to several tens of percent are common for all drag-derived densities. This is not different for GOCE.

During the course of the project, various aerodynamic models were compared for use in the density derivation, and a considerable uncertainty in density scale was encoun-

tered. Therefore, when the density data is to be compared to density model values or other density data sets, users of the data are advised to attempt to scale either the model or observed values for consistency. This is not necessary for studies of density variations with respect to a mean value, since research has shown that the effect of geometry model and aerodynamic model error on the variations is limited.

The true scale of thermospheric density is a topic of ongoing research, in which several members of the project team are involved. Therefore the possibility exists that the geometry and aerodynamic models for GOCE are updated for a later revision of the data, for improved consistency.

The reader is referred to the Validation Report and recent papers [e.g. March et al., 2018, 2019, Visser et al., 2019a,b], for more details.

### **2.2.3 Effect of thrust level variations at low thrust on density accuracy**

In an early phase of the study, it was established that the ion thruster on GOCE has a certain regime of low thrust levels, in which the thrust output is not as smooth as at lower or higher thrust levels. This phenomenon is apparently inherent in the design of the ion thruster. Due to the differences in the sampling and preprocessing of thruster activation data, it was not possible to further investigate the operation of the ion thruster in this regime with the help of accelerometer data. This thrust regime translates to density levels in the range of approximately  $17.5 \times 10^{-12}$  to  $22.5 \times 10^{-12}$  kg/m<sup>3</sup>, at which density and wind data in thermosphere data versions v1.4 and lower contained more noise-like variations, at the level of 3–4% RMS, compared to data from outside this range. In version 1.5 and later data, instead of the reported output thrust level, the input to the thruster was retrieved from the housekeeping data (the `thrust_demand` field was used instead of `current_thrust`). This has removed the variations with higher noise from the dataset. The current assumption is that the sample of the thrust input is a better representation of the average thrust level during the 8-second housekeeping data sampling interval than the sampled thrust output, containing this higher noise range.

### **2.2.4 Interpretation of the crosswind vector**

Note that due to limitations in the observation method, there is no possibility to retrieve the full wind vector from the accelerometer data. In the crosswind recovery, it has been assumed that the in-track wind is according to a model value, while the vertical component of the crosswind is zero. The fact that the crosswind is provided in a reference frame with components in the zonal (East), meridional (North) and vertical (Up) directions, does not mean that the measurements are to be interpreted as the full zonal or meridional winds.

Because of the near-polar orbit of GOCE, the crosswind direction is near to the zonal direction at low and mid latitudes, and reaches the meridional direction only at the instance of crossing the northernmost or southernmost latitudes.

To make a fair comparison of wind magnitudes with wind data from other sources (models or ground-based observations), it is therefore necessary to project the full wind data from these models or other measurements on the measured GOCE crosswinds. Similarly, if the crosswind data is to be used in models, they can only be used to constrain the wind component in the supplied direction.

### 2.2.5 Crosswind accuracy

The accuracy of crosswind measurements derived from satellite acceleration data was analysed by Doornbos et al. [2010]. The dominant source of errors in the crosswind data are due to acceleration errors in the spacecraft body-fixed Y-direction. These acceleration errors could be due to accelerometer bias, radiation pressure, and thruster activations in this direction. The level of these acceleration errors with respect to the aerodynamic acceleration determines the level of crosswind error. The low altitude of the GOCE satellite, at which aerodynamic accelerations are very high, is therefore a big advantage for obtaining high accuracy crosswind data. The Validation Report provides more information on this topic. A detailed error propagation study will be performed in the coming months, and the outcome of this study will likely be part of an updated version of the current data set and user manual.

### 2.2.6 Error estimates

Version 1.4 and later versions of the data add the results of an error propagation to the data set. These results are available per measurement, both in the time series data and in the gridd representation. The density and crosswind speed have been recomputed using a number of error sources. The differences between the densities and wind speeds with and without these errors have been added in a Root-Sum-Squared (RSS) sense. Note that the version 2.0 data uses a somewhat different error definition (according to Visser et al. [2019a]) than the earlier version 1.4 and 1.5 data. Note that not all possible error source have been taken into account. Therefore, the error estimates can not be assumed to represent accurate weighting factors when using the data in models. Nevertheless, the results of the error propagation can give valuable insight in relative density and wind data quality.

## 2.3 Vertical wind data

Vertical wind data is introduced in the version 2.0 data release. Details about the vertical wind retrieval algorithm and error sources are available in the following publications: Visser et al. [2019a,b]. Of particular importance is the fact that an accurate calibration of the vertical accelerations has proven difficult. The data has therefore been processed under the assumption that the long-term mean vertical acceleration was zero. This means that the data might not well represent long-term variability and absolute vertical wind values, but the variability of the vertical wind should be well-represented. Scientists who want to make use of the vertical wind data in publications are advised to contact Eelco Doornbos via [eelco.doornbos@knmi.nl](mailto:eelco.doornbos@knmi.nl).

## 2.4 Deorbit phase data

Two versions of the deorbit phase data are made available in the version 2.0 data release:

- DFACS channel data refers to a housekeeping telemetry data stream, containing acceleration data that has a wider dynamic range than the science channel telemetry stream. The advantage is that acceleration measurements have remained available

until closer to the actual re-entry, at higher levels of drag acceleration, before the instrument reached the limits of its dynamic range. A disadvantage of this stream is that it has not been filtered for certain signals introduced in the instrument and/or associated electronics, resulting in, for example, a sinusoidal pattern that is particularly noticeable in the vertical wind data. Another consequence is that this data set had to be independently calibrated from the rest of the mission's data.

- Density and wind based on GPS only acceleration data has been derived from GOCE GPS receiver data, using the FAST tool that is part of the DLR GHOST orbit determination software suite. No accelerometer data has been used in this product. The advantage of this is that data remains available up to the end of continuous telemetry, approximately 7 hours before re-entry. In fact, the GPS-derived accelerations become more accurate as the accelerations become larger, while the accelerometer data starts to saturate and becomes unusable at lower altitudes.

Due to these particularities of the deorbit phase data, scientists who want to make use of this data are advised to contact Eelco Doornbos (via [eelco.doornbos@knmi.nl](mailto:eelco.doornbos@knmi.nl)), before making use of the data in publications.



# Bibliography

- Bruce R. Bowman, W. Kent Tobiska, Frank A. Marcos, Cheryl Y. Huang, Chin S. Lin, and W.J. Burke. A new empirical thermospheric density model JB2008 using new solar and geomagnetic indices. *Draft for CIRA 2008*, 2008.
- Bruinsma, Sean. The dtm-2013 thermosphere model. *J. Space Weather Space Clim.*, 5:A1, 2015. doi:10.1051/swsc/2015001. URL <http://dx.doi.org/10.1051/swsc/2015001>.
- Eelco Doornbos, Jose van den IJssel, Hermann Lühr, Matthias Förster, and Georg Koppenwallner. Neutral density and crosswind determination from arbitrarily oriented multiaxis accelerometers on satellites. *Journal of Spacecraft and Rockets*, 47(4): 580–589, 2010. doi:10.2514/1.48114.
- G March, E N Doornbos, and P N A M Visser. High-fidelity geometry models for improving the consistency of CHAMP, GRACE, GOCE and Swarm thermospheric density data sets. *Advances in Space Research*, July 2018. doi:10.1016/j.asr.2018.07.009. URL <https://linkinghub.elsevier.com/retrieve/pii/S0273117718305714>.
- Günther March, Tim Visser, Pieter Visser, and Eelco Doornbos. CHAMP and GOCE thermospheric wind characterization with improved gas-surface interactions modelling. *In preparation for submission to Advances in Space Research*, 2019.
- J.M. Picone, A.E. Hedin, D.P. Drob, and A.C. Aikin. NRLMSISE-00 empirical model of the atmosphere: Statistical comparisons and scientific issues. *Journal of Geophysical Research*, 107(A12), 2002. doi:10.1029/2002JA009430.
- M.F. Storz, B.R. Bowman, J.I. Branson, S.J. Casali, and W.K. Tobiska. High accuracy satellite drag model (HASDM). *Advances in Space Research*, 36(12):2497–2505, 2005.
- T Visser, G March, E Doornbos, C de Visser, and P Visser. Horizontal and vertical thermospheric cross-wind from GOCE linear and angular accelerations. *Advances in Space Research*, January 2019a. doi:10.1016/j.asr.2019.01.030. URL <https://linkinghub.elsevier.com/retrieve/pii/S027311771930050X>.
- Tim Visser, Eelco N Doornbos, Coen C de Visser, Pieter N A M Visser, and Bent Fritsche. Torque model verification for the GOCE satellite. *Advances in Space Research*, 62(5):1114–1136, September 2018. doi:10.1016/j.asr.2018.06.025. URL <https://linkinghub.elsevier.com/retrieve/pii/S027311771830509X>.
- Tim Visser, Günther March, Eelco Doornbos, Coen de Visser, and Pieter Visser. Characterization of thermospheric vertical wind activity using goce data and validation against explorer missions. *Under review at Journal of Geophysical Research: Space Physics*, 2019b.